International Journal of Electrical and
Electronics Engineering Research (IJEEER)
ISSN(P): 2250-155X; ISSN(E): 2278-943X
Vol. 5, Issue 6, Dec 2015, 19-30

ROUTE-TO-CHAOS AND OPERATION OF LASER DIODE UNDER OPTICAL FEEDBACK WITH LINEWIDTH ENHANCEMENT FACTOR

SALAH ABDULRHMANN[1] & A. AL-HOSSAIN[2]

[1]Department of Physics, Faculty of Science, Assiut University, Assiut, Egypt

[1]Department of Physics, Faculty of Science, Jazan University, KSA,

[2]Department of Mathematics, Faculty of Science, Jazan University, KSA

ABSTRACT

This paper investigates numerically influence of linewidth enhancement factor and injection current on the type of the route-to-chaos and associated operation states of laser diodes under external optical feedback. The study is based on numerical solutions of a time-delay model of rate equations, and the solutions are employed to construct bifurcation diagrams and to examine the output time fluctuations and phase portraits of the laser. The simulation results show that linewidth enhancement factor causes significant changes in the route-to-chaos and the laser states. The state of the laser is identified into six distinct regimes, namely, continuous wave, periodic oscillation, period doubling or two, period-three, period-four oscillations and chaos, which is depending on the value of the linewidth enhancement factor, feedback strength and injection current level. The route-to-chaos is period-four when linewidth enhancement factor is less than or equal to three. The route is period-three when linewidth enhancement factor increases up to 7. The feedback strength when the laser transits from continuous wave to periodic oscillation, period doubling or chaos state decreases with the increase in the linewidth enhancement factor. Decreasing the injection current and increasing the linewidth enhancement factor stimulating the laser to operate in continuous and periodic oscillations.

KEYWORDS: ***Laser Diodes, Linewidth Enhancement Factor, Optical Feedback, and Chaos***

Received: Oct 10, 2015; **Accepted:** Oct 20, 2015; **Published:** Oct 28, 2015; **Paper Id.:** IJEEERDEC20153

Original Article

1. INTRODUCTION

Laser diodes (LDs) such as InGaAsP/InP lasers emitting at 1.2-1.6 μm are widely used as light sources for long-distance optical communication systems [1]. The operation states and route-to-chaos of such lasers are strongly modified by optical feedback (OFB) from an external reflector. The variation of the operation states and types of the route-to-chaos of LDs depend on various factors, which divided into (i) internal parameters, such as nonlinear gain (NLG) and nonradiative recombination life time (NRRLT); and others, and (ii) external parameters, such as OFB strength, external cavity length and injection current. While weak OFB levels result in linewidth narrowing and improved frequency stability, moderate to strong OFB levels might induce the laser to switch to a state of significant spectral broadening and dynamical complexity, which has been called "coherence collapsed state" or chaos [1-4].

However, the operation and states characteristics of the LD are influenced by the linewidth enhancement factor (LEF), also known as α–factor, which has a great importance for LDs, as it is one of the main features that

distinguish the behavior of LDs with respect to other types of lasers. The LEF influences several fundamental aspects of LDs, such as the linewidth, the chirp under current modulation, the mode stability, the occurrence of filamentation in broad–area devices. In synthesis, the dynamics of LDs is greatly influenced by the LEF, which is of particular interest for the study of injection phenomena, OFB effects, and mode coupling as occurring in VCSELs [5-14].

The route-to-chaos is one of the interesting nonlinear phenomena associated with OFB; it may include dynamics with period-doubling (PD), sub-harmonics (SH) or quasi-periodicity (QP) [15-17]. PD is observed in the limit of short-external cavity [16, 17]; it follows a region of periodic oscillation (PO) and is characterized by the PO frequency and its half harmonic. Kao et al. [16] predicted that this frequency should correspond to Hopf-bifurcation (HB) point (the onset of PO). SH transitions to chaos were predicted as an intermediate state from PD to QP associated with increasing the external-cavity length [16]. It is characterized by the HB frequency and one of its rational SH, and it is followed by mode locking with these frequencies [16]. Ahmed et al. [18] used the ratio of the relaxation frequency to the external-cavity resonance frequency to classify the route-to-chaos in LDs. They showed that the route is PD when the frequency ratio is less than unity. The route becomes SH with the periodic oscillation frequency when the ratio is higher than unity and less than 2.25. When the ratio exceeds 2.3, the route is QP characterized by the compound-cavity frequency and the relaxation frequency as well as their frequency difference [18]. Abdulrhmann et al. [19-21] investigated the influence of NLG and NRRLT on the operation states, route-to-chaos and noise of LDs. He showed that, the value of the OFB rate at which the transition from CW to PO or chaos state occur increases, as the intensity of the NLG/NRRLT is increased/decreased. Under strong OFB, the increase/decrease in the NLG/NRRLT causes change of chaotic dynamics to PO or CW operation depending on OFB strength [19, 20]. The relative intensity noise is found to be as low as the quantum noise level when the laser is operated in CW or PO region and at relatively large/small values of the NLG/NRRLT [21].

However, based on our knowledge, there is no report that studied the effect of LEF, OFB strength and injection current ratio on the route-to-chaos characteristics and associated states of operation for LDs. In this article, we apply the time-delay rate equation model in [18, 22] of OFB in LDs to study influence of LEF on the route-to-chaos and associated laser operation. In such a model, OFB is treated as time delay of the laser radiation due to multiple roundtrips between the laser front facet and the external mirror. Intensive computer simulations are run to investigate the operation and dynamics of 1550-nm InGaAsP/InP LD with a short external cavity using a wide range of injection current. The route-to-chaos and associated laser operation is classified in terms of the bifurcation diagrams of the peak value of the photon number at each feedback strength and injection current. We identified the operation states of LD into six distinct operating regimes, namely, continuous wave (CW), PO, PD, period-three (3xP) and period-four (4xP) route-to-chaos and coherence collapse or chaos depending on the value of the LEF, OFB strength and injection current ratio. The results show that, variation of LEF cause significant changes in the route-to-chaos and operation states of the laser. The value of the OFB strength at which the transition from CW to PO or chaos state occur decreases, as the value of the LEF is increased. Under lower values of injection current and by increasing LEF, the laser operation states are only CW and PO states and there is no chaos state. At lower values of the injection current, highest LEF works in such a way to induce CW and PO operations.

The paper is organized as follows; in sec. 2 the time-delay rate equation model of LD with OFB is introduced. These rate equations are solved numerically in Sec. 3. In Sec. 4, the bifurcation diagrams of the photon number of LD over wide ranges of LEF and injection current are shown. The time variations of the photon numbers and phase portrait of the induced route-to-chaos states of operation are also presented. The conclusions are presented in Sec. 5.

2. THEORETICAL MODEL OF SIMULATION

In this paper, we apply the model in [18] to investigate the effect of the LEF on the operations, and route-to-chaos of InGaAsP/InP laser over wide ranges of the OFB strength and injection current. The time-delay rate equations of the photon number $S(t)$, optical phase $\theta(t)$ and carrier number $N(t)$, which describing the LD dynamics are formulated as

$$\frac{dS}{dt}=\left\{\frac{a\xi}{V}(N-N_g)-BS-G_{th0}+\frac{c}{n_D L_D}\ln|T|\right\}S+\frac{a\xi}{V}N, \tag{1}$$

$$\frac{d\theta}{dt}=\frac{\alpha a\xi}{2V}(N-\bar{N})-\frac{c}{2n_D L_D}(\varphi-\bar{\varphi}), \tag{2}$$

$$\frac{dN}{dt}=-\frac{a\xi}{V}(N-N_g)S-\frac{N}{\tau_S}+\frac{I}{e}, \tag{3}$$

where $a\xi(N-N_g)/V$ is the linear gain coefficient with a and N_g as material constants and ξ as the confinement factor of the optical field into the active region of volume V. α is the linewidth enhancement factor (LEF), and I is the injection current and $\bar{N}$ is the corresponding time averaged electron number. G_{th0} is the threshold gain level, which is determined by the loss coefficient k of the laser and mirror loss:

$$G_{th0}=\frac{c}{n_r}\left\{k+\frac{1}{2L}\ln\frac{1}{R_f R_b}\right\}, \tag{4}$$

Various models have been advanced to account for gain nonlinearities based on the density-matrix theory [24-28]. In this paper, the nonlinear phenomenon of NLG is included in the rate equations in terms of coefficient B, which is given in the third-order perturbation theory of gain by [23, 24].

$$B=\frac{9\hbar\omega_o}{4\varepsilon_o n_D^2}\left(\frac{\tau_{in}}{\hbar}\right)^2\left(\frac{\xi}{V}\right)^2 a|R_{cv}|^2(N-N_s)=B_c(N-N_s), \tag{5}$$

where R_{cv} is the dipole moment, τ_{in} is the intra-band relaxation time and N_s is an injection level characterizing the NLG. The electron lifetime which should account for the non-radiative recombination by Auger processes since they have an effective contribution to the lasing mechanism in long wavelength laser is τ_s, which is defined as [25]

$$\frac{1}{\tau_s}=A_{nr}+B_r(N/V)+C_{AUG}(N/V)^2, \tag{6}$$

where A_{nr}, is a coefficient for the nonradiative contribution arising from crystal impurities, B_r is the radiative decay coefficient, and C_{AUG} is a decay coefficient due to Auger processes [25]. The complex coefficient T describes the influence of OFB on the threshold conditions are given by [18, 22]:

$$T=1-\sum_{m=1}(K_{ex})^m\left(\frac{R_f}{1-R_f}\right)^{m-1}\exp\{-jm\psi\}\frac{S(t-m\tau)}{S(t)}=|T|\exp\{-j\phi\}. \tag{7}$$

where, m is an index for the round-trip, ψ is a phase term combining the phase changes due to reflection by the external

mirror, R_{ex}, n_{ex} and L_{ex} are the external mirror power reflectivity, refractive index and length of the external cavity, respectively. The combined phase ψ is defined in terms of the phase retarded due to reflection by the external mirror ϕ_{ex}, front facet, ϕ_f, and due to a round-trip in the fiber cavity $\omega\tau$, as $\psi=\phi_{ex}+\phi_f+\omega\tau$, where ω is the emission circular frequency and $\tau = 2n_{ex}L_{ex}/c$ is the round-trip time. The strength of OFB is measured by the coefficient K_{ex}, which is determined by the ratio of the external reflectivity R_{ex} to the front-facet reflectivity R_f as,

$$K_{ex} = (1-R_f)\sqrt{\eta\frac{R_{ex}}{R_f}} \tag{8}$$

where η is the coupling ratio of the injected light into the laser cavity. The argument ϕ of the complex OFB function T is obviously given by:

$$\phi = -\tan^{-1}\left\{\mathrm{Im}[T]/\mathrm{Re}[T]\right\} + \ell\pi \tag{9}$$

where ℓ is an integer. Determining the value of ϕ in the two-dimensional space (*Re[T]-Im[T]*) depends on both the signs and magnitudes of *Re[T]* and *Im[T]*.

3. PROCEDURES OF NUMERICAL CALCULATIONS

Equations (1)-(3) are solved numerically with the fourth-order Runge-Kutta method. The simulation model is applied to InGaAsP/InP lasers emitting in the wavelength of 1550 nm. The time step of integration is set as Δt=5 ps, which is short enough to get good resolution of the time variation of the photon number. The integration was carried out over a period of 6 μs, which is long enough to achieve stable dynamics of the laser. The injection current is varied between 1.05 I_{th0} and 2.0 I_{th0}, where I_{th0} = 10.8 *mA* is the threshold current of the solitary laser. The influence of OFB is taken in terms of the strength of OFB K_{ex}. The integration was first made without OFB (the case of the solitary laser) from time t = 0 until the first round trip time τ, i.e., putting K_{ex}=0 and $\varphi = 0$ in the rate equations. The calculated values of *S(t)* and θ*(t)* are then stored for use as time delayed values *S(t-*τ*)* and θ*(t-*τ*)* for the further integration of rate equations (1)-(3) including the feedback terms. We include three round trips (m=5). The calculated values of *S(t*=0 to τ*)* and θ*(t*=0 to τ*)* are then stored for use as time delayed values *S*(*t-* τ) and θ(*t-* τ) for integration of the rate equations over the period t=2τ to 3τ including OFB terms. Then the calculated values *S*(*t-*τ), *S*(*t-*2τ), θ(*t-*τ), and θ(*t-*2τ) are used as time delayed values for integration over the period t=2τ to 5τ. Starting from this time, the integration is proceeded over a long period of time T=4–6 μs by considering all terms of *S*(*t-m*τ) and θ(*t-m*τ), m=0,1,2, 3, as time delayed values. The value of the combined phase change ψ is set to be ψ= *0.0*, and the value of the external cavity length is set to be L_{ex}= 0.03 m in the present calculations. The phase φ of the feedback light was chosen to vary continuously for time evolution because the solution of arc tangent is limited in the range of $-\pi/2$ to $\pi/2$ in the computer work. The averaged values $\overline{\varphi}$ are set as zero in this paper. The applied numerical values of InGaAsP/Inp lasers are given in table 1 in Ref. [19].

4. RESULTS AND DISCUSSIONS

In order to understand the effect of the LEF on the behavior of the external cavity LDs, we simulate the laser dynamics over wide ranges of the LEF, the OFB strength (in terms of K_{ex}) and injection current ratio.

4.1. Bifurcation Diagrams Analysis

Investigation of the influence of LEF on the route-to-chaos of the laser is done by simulating the bifurcation diagrams of the photon numbers $S(t)$ in terms of the OFB strength K_{ex} and injection current ratio I/I_{th0}. The bifurcation diagrams, which constructed by plotting the peak(s) of the temporal trajectory of the photon number $S(t)$ at each level of OFB strength K_{ex}, and at three values of the injection current ratio, I/I_{th0} = 1.05 (near the threshold), 1.5 (well above the threshold) and 2.0 (far from the threshold) and at four values of LEF, α = 1.0, 3.0, 5.0 and 7.0, are plotted in figures 1-3, respectively. The results are normalized by the time ensemble average $\bar{S}$. In these figures, we are interested in exploring an overview of the LD operation over a wide range of the LEF, injection current and OFB strength.

General features of these diagrams are as follows. Under very weak OFB, the solution of the rate equations is still stationary and the laser operates in CW operation for which no points are plotted in the figure. With the increase in OFB strength, K_{ex}, this stationary solution bifurcates first into a stable limiting cycle characterizing periodic oscillation (un-damped relaxation oscillation), which is represented by a single point in the diagram. The starting point of the bifurcation is called a Hopf-bifurcation (HB) point and is characterized by frequency $f_{po(H)}$, which is not necessarily equal to the relaxation oscillation frequency f_{r0}, and as indicated in the Figures 1 (a to d) by first arrow (black arrow) is moved toward decreasing OFB strength K_{ex} from 0.028 to 0.0064 by increasing LEF from 1.0 to 7.0, respectively.

With further increase in OFB, the solution of the rate equations bifurcates into a torus (multiple bifurcation points) followed by a chaotic state, and then the laser is attracted again to CW operation. As shown in the figures 1-3, the torus is PD in which periodic oscillation bifurcates first into two branches, where the trajectory of $S(t)$ has two peaks of different heights in every two successive periods, which indicated in the Figures 1 (a to d) by second arrow (blue arrow) in which PO bifurcates first into two branches. With the increase in K_{ex}, the oscillation period is multiplied to more than twice and the laser is attracted to transition to coherence collapse or chaos, which indicated in the Figures 1 (a to d) by fourth arrow (red arrow). When LEF α = 1 and 3, the route-to-chaos is 4xP as indicated in the Figures 1 (a, and b) by third arrow (green arrow), respectively. In Figures 1(c and d), and when LEF, α = 5 and 7, the route-to-chaos is 3xP (green arrow). Then by increasing the LEF the route-to-chaos of the laser changes from 4xP route-to-chaos to 3xP route-to-chaos.

Effect of the injection current on the states and route-to-chaos of the LD at several values of LEF is shown in Figures 2 and 3. Well above the threshold current I_{th0}, at I/I_{th0} = 1.5, the states and route-to-chaos is changed from 4xP to PO route-to-chaos when α = 1.0 and from 3xP to 4xP route-to-chaos when α = 7.0 as shown if Figures 2 (a, and d), respectively. By decreasing the injection current to I/I_{th0} = 1.05 (near threshold), the laser operates in CW and PO and there is no chaos state, especially at higher values of LEF as shown in Figures 3(a-d). With the decrease in I/I_{th0}, the laser operation changes to CW and PO at all values of the LEF, and then the laser is attracted to transition to CW operation by increasing the OFB strength.

In the following subsection, we characterize the three types of route-to-chaos when I/I_{th0} = 2.0 in terms of the time variation of photon numbers $S(t)$ and corresponding phase portraits of the state of the LD.

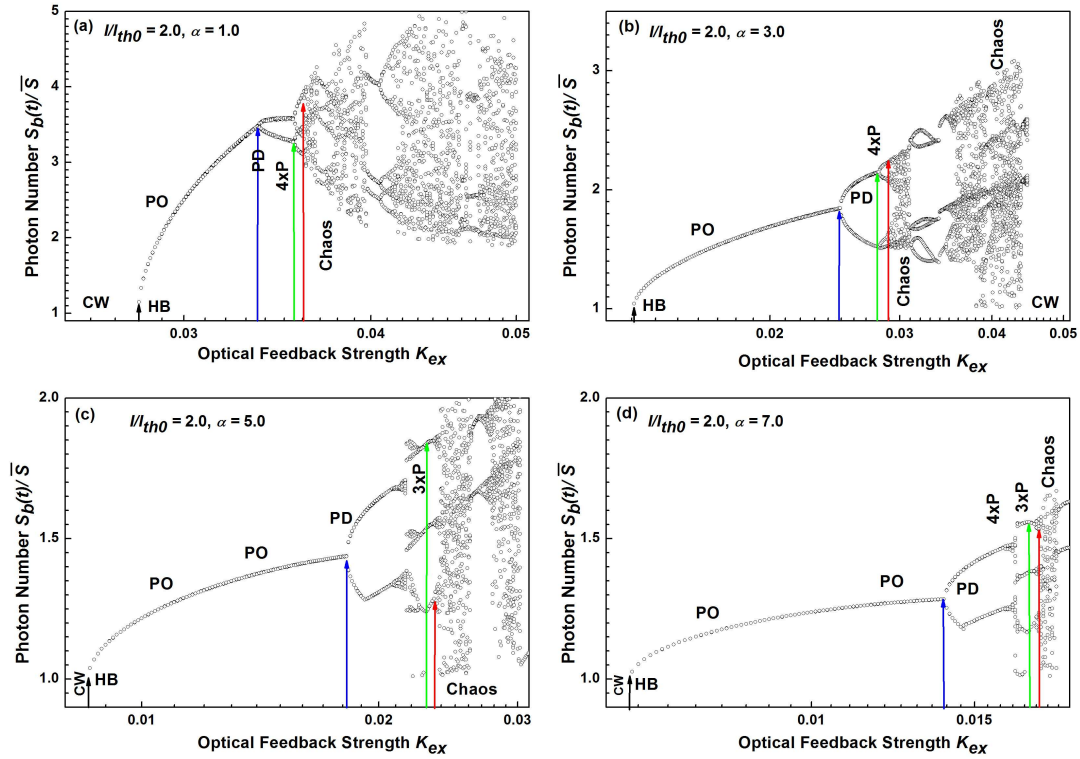

Figure 1: Bifurcation diagrams of a LD under OFB when I/I_{th0} = 2.0 (a) α = 1.0, (b) α = 3.0, (c) α = 5.0 and (d) α = 7.0

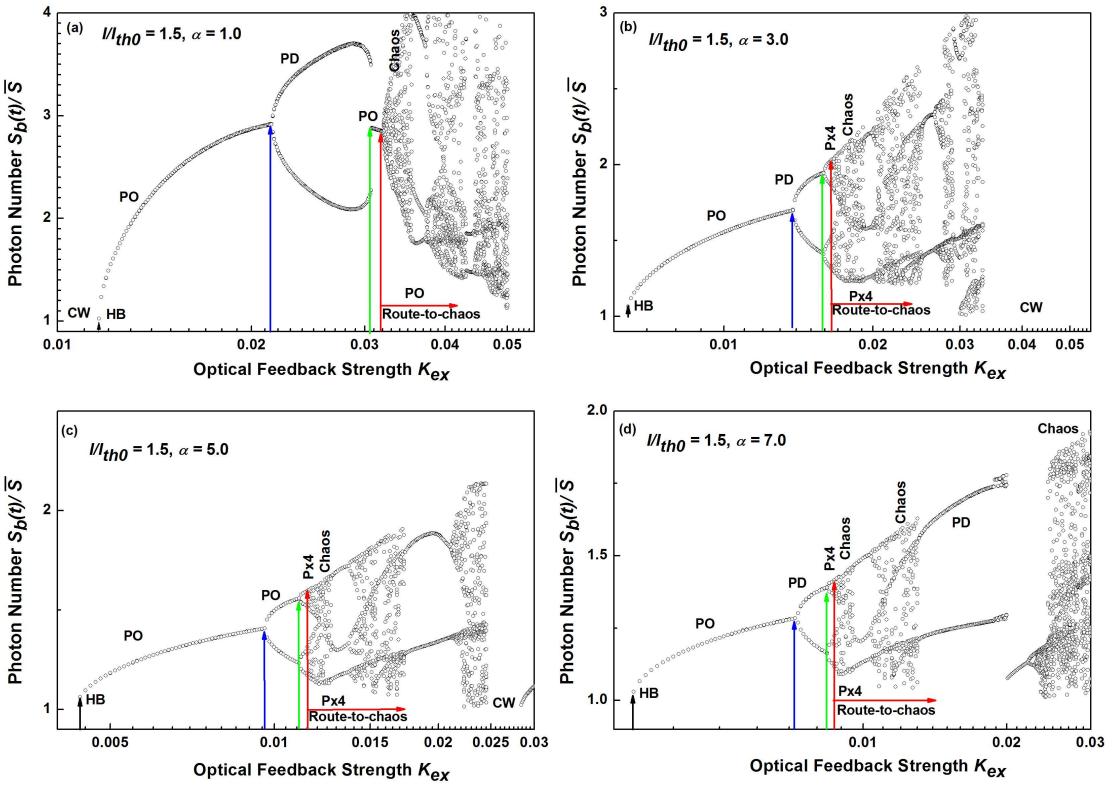

Figure 2: Bifurcation diagrams of a LD under OFB when I/I_{th0} = 1.5 (a) α = 1.0, (b) α = 3.0, (c) α = 5.0 and (d) α = 7.0

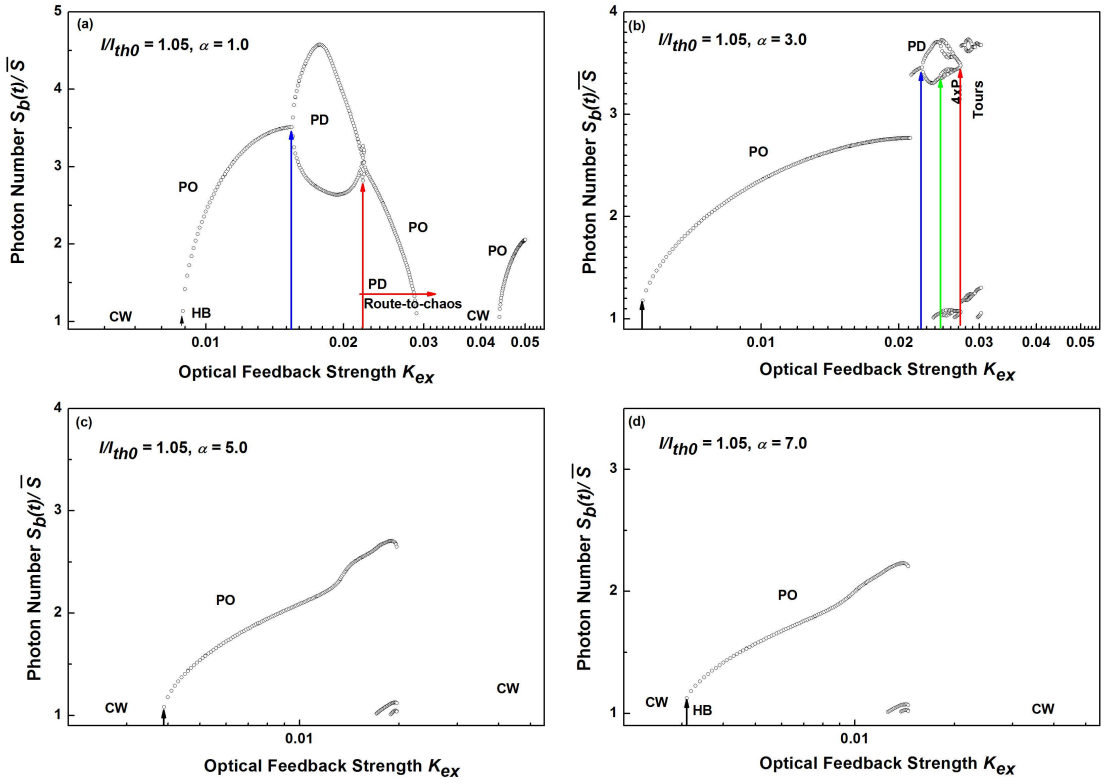

Figure 3: Bifurcation diagrams of a LD under OFB when I/I_{th0} = 1.05 (a) α= 1.0, (b) α= 3.0, (c) α= 5.0 and (d) α= 7.0

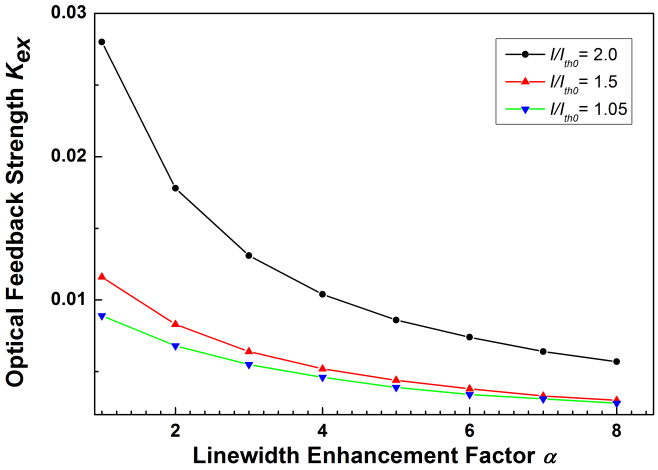

Figure 4: Dependencies of the OFB strength K_{ex} at HB ppoint on the LEF α at iinjection ccurrent rratio I/I_{th0} = 1.05, 1.5, and 2.0

The feedback level when a PO appears at HB point calculated from the numerical simulation of the rate equations using bifurcation diagrams shown in figures 1-3, as a function of the LEF is shown in figure 4. Notice that they are almost nonlinear functions (exponential decay) of LEF, which means that increasing the LEF decreases the feedback level required to destabilize a PO, PD, … or a chaos state. Figures 1-3 and 4, demonstrate that, decreasing the LEF renders a steady state more stable by increasing the feedback level above. By decreasing the LEF, the level of the OFB strength corresponding to a HB point and route-to-chaos increases, which leads to increasing in the laser threshold current. We believe that, from the result shown in Figures 1-3 and 4, the instability of the LD can be reduced by decreasing the LEF

and decreasing the injection current ratio to values near from the threshold and increasing OFB strength, which helps to design a laser diode with high static and dynamic performance. So, it is clear that from Figures 1-3 and 4, any increase in the LEF leads to increase in the threshold current [8]. And any increase in the OFB strength reduces the total cavity loss of the laser diode [26], which caused to increase the photon lifetime and increase the threshold carrier density, which increase the laser threshold current. Thus, from the physical and practical point of view, any increase in the laser threshold current leads to increase in the laser stability. These results support our conclusion that, at higher values of LEF and when the injection current be near the threshold the laser stability is improved and moves toward stable operations.

In the following sections, we characterize the operation states of the laser and the two types of route-to-chaos in terms of the time variation of photon number *S(t)*, and corresponding phase portraits for various states of the laser.

4.2. Time Variations of *S(T)* and Phase Portraits at Several States of the LD

In this section, we examine the time variation of photon number from back facet *S(t)* and phase portrait of LD of the operation states of LD till reach to chaos shown in Figures. 5 and 6 at I/I_{th0} =2.0 and at three values of the LEF α = 3.0, 5.0 and 7.0. The examination is done over a wide range of the operation states (PO, PD, and 3xP, 4xP route-to-chaos, and chaos).

The simulated time variations of the photon number *S(t)*, of PO operation of the laser at K_{ex}= 0.02, 0.015, and 0.01 and when α = 3.0, 5.0 and 7.0 are shown in Figures 5 (a, e, and i). The time variation of the PO laser operation exhibits uniform fluctuation with period-one. Theses PO states are confirmed by plotting the corresponding phase portrait in Figures 6 (a, e, and i), The phase portraits are characterized by limit cycle attractor (period-one oscillation). By increasing K_{ex} to 0.027, 0.02 and 0.015, which represent the regions of the PD operation, the laser operation becomes more complicated and the time variation becomes with period-two, which could be considered a kind of PD oscillations as shown in Figures. 5 (b, f, and j). Figures 6 (b, f, and j) show the phase portrait of PD operations, which are characterized by limit cycle attractor (period-two oscillation). When K_{ex}= 0.0284, 0.023, and 0.017, the system nonlinearity increases irregularities of *S(t)* attracting the laser oscillation into route-to-chaos as shown in Figures 5(c, g, and k). As shown in Figures. 5 (c) the time fluctuations of *S(t)*, induce four peaks, which represent 4xP route to chaos and this is confirmed by the phase portrait shown in Figure. 6 (c), which is characterized by limit cycle (period-four) attractor. By increasing LEF to 5.0 and 7.0 the route to chaos is changed to 3xP as shown in Figures 5 (g and k), the time fluctuations induce three peaks and the phase portrait is characterized by limit cycle (period-three) attractor as shown in Figures 6 (g and k). When (K_{ex}=0.03, 0.025, and 0.018), the laser state becomes more complicated and enter to coherence collapse or chaos regime. Figures 5 (d, h, and l), shows non-uniform or random fluctuations of the time variation of *S(t)*, which is appeared as a chaotic attractor in the phase portrait shown in Figures 6 (d, h, and l).

CONCLUSIONS

We investigated the influence of LEF on the states and route-to-chaos of LDs. The simulations were applied to 1550-nm In GaAsP/InP lasers over a wide range of the injection current. The route-to-chaos and the associated laser operations are classified by the bifurcation diagrams of the photon number, time-variations of the photon number. The simulation results show that, LEF cause significant changes in the operation states and the route-to-chaos of the lasers. We find that the values of the feedback rate at which the transition from CW to periodic oscillation or coherence collapsed or chaos state occurs decreases, as the LEF is increased. We identified the operation states of SL into six distinct operating

regimes, namely, CW, PO, PD, before route-to-chaos and 3xP and 4xP route-to-chaos and coherence collapse or chaos depending on the value of the LEF and OFB strength. The route-to-chaos is 4xP when LEF is less than or equal to three. The route is 3xP when LEF increases up to 7. The OFB strength when the laser transits from CW to PO or PD or chaos state decreases with the increase in the LEF. When the SLs operated under OFB and by decreasing the values of the LEF, the operations of the laser change from chaos operation to PO or CW operation, which is more stable and desirable. At higher values of LEF and when the injection current be near the threshold the laser stability is improved and moves toward stable operations. Finally we expect that SL subject to OFB exhibits much more stability under lower or higher values of LEF depending on the values of the injection current.

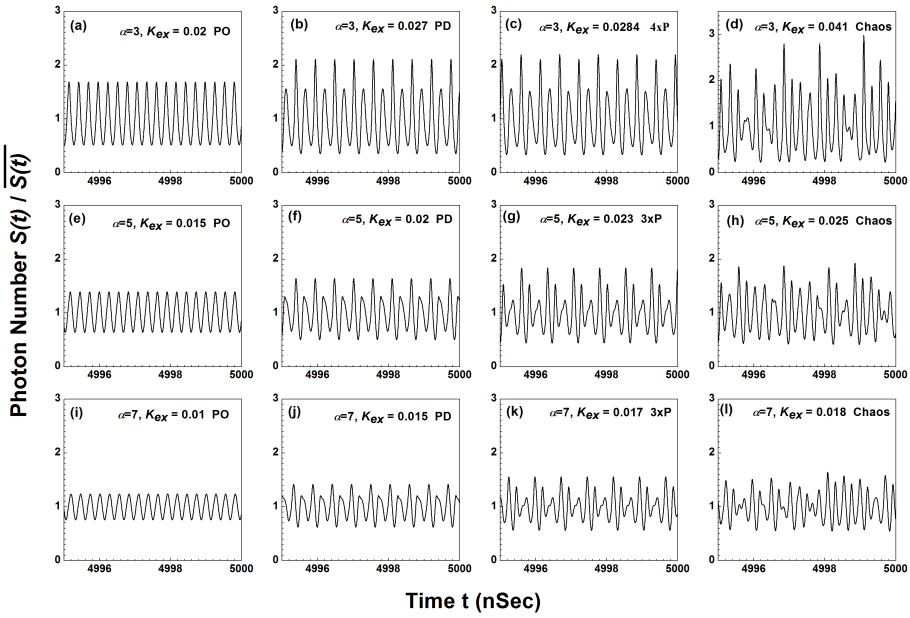

Figure 5: Time Variations of Photon Number S(t)at I/I_{th0}= 2.0 and at α= 3.0, 5.0, and 7.0

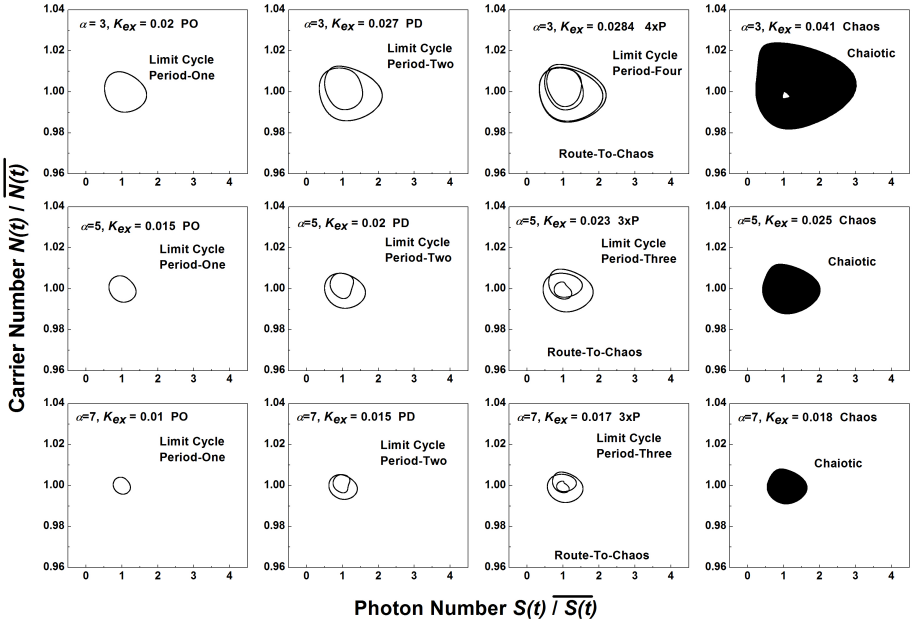

Figure 6: Phase Portraits of a LD at at I/I_{th0}= 2.0 and at α= 3.0, 5.0, and 7.0

ACKNOWLEDGEMENTS

The authors would like to thank the Deanship of Scientific Research, Jazan University and SABIC Corporation for partial support of the present research work.

REFERENCES

1. *G. P. Agrawal. (2003). Optical Fiber Communication Systems, Chapter 6. Van Nostrand Reinhold, New York.*
2. *Y. Kitaoka et al. (1996). Intensity noise of laser diodes with optical feedback. IEEE J. Quantum Electron., 32, 822*
3. *K. I. Kallimani, et al. (1998). Relative intensity noise for laser diodes with arbitrary amounts of optical feedback. IEEE J. Quantum Electron., 34, 1438*
4. *Safwat W.Z. Mahmoud, et al. (2013). Comprehensive large-signal analysis of RF modulation of vertical cavity surface emitting lasers. Optics & Laser Technology, 45, 406*
5. *C. H. Henry, (1982). Theory of the linewidth-enhancement factor of semiconductor lasers. IEEE J. Quantum Electron., QE-18, 259*
6. *Osinski and J. Buss, (1987). Linewidth broadening factor in semiconductor lasers—An overview. IEEE J. Quantum Electron., 23, 9*
7. *C. Masoller and N. B. Abraham, (1998). Stability and dynamical properties of the coexisting attractors of an external-cavity semiconductor laser. Phys. Rev. A, 57, 1313*
8. *D. Rodriguez, et al. (2005). Gain, index variation, and linewidth-enhancement factor in 980-nm quantum-well and quantum-dot lasers. IEEE J. Quantum Electron., 41, 117*
9. *A.T. Ryan, et al. (1994). Optical-feedback-induced chaos and its control in multimode semiconductor lasers. IEEE J. Quantum Electron., 30, 668.*
10. *Z. Mi, et al. (2005). High-speed 1.3 μm tunnel injection quantum-dot lasers. Appl. Phys. Lett., 86, 153109.*
11. *Z. Mi and P. Bhattacharya, (2007). Analysis of the linewidth-enhancement factor of long-wavelength tunnel-injection quantum-dot lasers. IEEE J. Quantum Electron., 43, 363.*
12. *S. Abdulrhmann, (2012). Dynamics and Noise of Pumping Lasers Affected by the Line-width Enhancement Factor. TURKISH JOURNAL OF PHYSICS, 36, 225.*
13. *Najm M. AL-HOSINY, (2014). Effect of Linewidth Enhancement Factor on the Stability Map of Optically Injected Distributed Feedback Laser. OPTICAL REVIEW, 21, 261*
14. *Chao-Fu Chuang, et al. (2014). Linewidth enhancement factor in semiconductor lasers subject to various external optical feedback conditions. OPTICS EXPRESS, 22, 5651.*
15. *J. Mork et al. (2002). Route-to-chaos and competition between relaxation oscillations for a semiconductor laser with optical feedback. Physics Review Letters. 65, 1999*
16. *Kao YH et al. (1994). Mode description of routes to chaos in external-cavity coupled semiconductor lasers. IEEE Journal of Quantum Electronics. 30, 1732*
17. *Ryan AT et al. (1994). Optical-feedback-induced chaos and its control in multimode semiconductor lasers. IEEE Journal of Quantum Electronics. 30, 668*
18. *M. Ahmed, et al. (2009). Numerical modeling of the route-to-chaos of semiconductor lasers under optical feedback and its*

dependence on the external cavity length. International Journal of Numerical Modelling: Electronic Networks, Devices and Fields, 22, 434

19. *S. Abdulrhmann, (2013). Influence of Nonlinear Gain on the Onset of Chaos, States and Dynamics of Laser Diode with Optical Feedback. International Journal of Electrical and Electronics Engineering Research (IJEEER), 3, 27.*
20. *S. Abdulrhmann, (2013). Rout to Chaos and Nonradiative Recombination in Laser Diode. International Journal of Semiconductor Science & Technology (IJSST), 3, 1*
21. *S. Abdulrhmann and A. Al-Hossain, (2014). Variations of Operations and noise of Semiconductor Lasers subject to Optical Feedback with Nonlinear Gain and Nonradiative Recombination. AIP Conference Proceedings 1653, 020002, 4th International Advances in Applied Physics and Materials Science Congress and Exhibition (APMAS-14), Fethiye- Mugla, Turkey, 24-27 April 2014.*
22. *S. Abdulrhmann et al. (2003). An improved analysis of semiconductor laser dynamics under strong optical feedback. IEEE Journal of Selected Topics on Quantum Electronics., 9, 1265*
23. *M. Ahmed and M. Yamada, (1998). An infinite order perturbation approach to gain calculation in injection semiconductor lasers. J. Appl. Phys., 84, 3004*
24. *M. Yamada and Y. Suematsu, (1981). Analysis of gain suppression in undoped injection lasers. J. Appl. Phys., 52, 2653*
25. *Robert Olshansky et al. (1984). Measurement of radiative and nonradiative Recombination rates in InGaAs light sources. IEEE J. Quantum Electron., QE-20, 838*
26. *G. H. M. Tartwijk and D. Lenstra. (1995). Semiconductor lasers with optical feedback and optical injection. Quantum and SemiclassicalOptics: Journal of the European Optical Society, Vol.7, 87-144*